Mathematical modeling for facilitated transport of Ge(IV) through supported liquid membrane containing Alamine 336

Hossein Kamran Haghighi [a], Mehdi Irannajad *[a], Agustin Fortuny [b], Ana Maria Sastre [c]

[a] *Department of Mining and Metallurgy, Amirkabir University of Technology, Tehran, Iran*

[b] *Department of Chemical Engineering, Universitat Politècnica de Catalunya, EPSEVG, Av. Víctor Balaguer s/n, 08800 Vilanova i la Geltrú, Spain.*

[c] *Department of Chemical Engineering, Universitat Politècnica de Catalunya, ESTEIB, Av. Diagonal 647, 08028 Barcelona, Spain.*

* Corresponding author: iranajad@aut.ac.ir

Abstract

A mathematical model was developed for the germanium facilitated transport from a medium containing tartaric acid using Alamine 336 as a carrier. Modeling was carried out based on the extraction constant (K_{ext}) obtained from the liquid-liquid extraction (LLX) modeling. The LLX data was achieved from experiments with conditions being Alamine 336 concentrations of 0.1-10 %v/v from a solution containing about 1.378 mmol/L Ge (100 mg/L) and tartaric acid as an anionic complexant. The LLX model was attained using the equilibrium-based procedure and fitted to extraction experimental data for various carrier concentrations. This model presented an accurate extraction constant (K_{ext}=0.02) used in the facilitated transport modeling. The flat sheet supported liquid membrane (FSSLM) experiments were conducted in the condition of 1.378 mmol/L Ge (100 mg/L), tartaric acid concertation of 2.760 mmol/L, 1 M HCl as a stripping phase and various Alamine 336 concentrations in the range of 0 to 35 %v/v. The FSSLM model was developed according to the Fick's law, the diffusional transport, and equilibrium equations. According to the model, mass transfer and diffusion coefficients for various concentrations of the carrier were found. In addition, the calculated and experimental values had a good correlation with together showing the validity of the model. This model can be used in the further process simulation such as hollow fiber SLMs.

Keywords: Germanium; Supported liquid membrane; Diffusion; Mathematical modeling; Transport

Introduction

Liquid membrane techniques, especially supported liquid membranes (SLMs), have been increasingly used for treating and purifying solutions in hydrometallurgical industries Benzal et al. (2004); (Bhatluri et al. 2015; Chaturabul et al. 2015; Duan et al. 2017b; Hosseini et al. 2016; Kaya et al. 2013; Mokhtarani et al. 2015; Peydayesh et al. 2013; Wang et al. 2015). Germanium is a metalloid that may exist in wastewaters and effluents of coal fly ash and zinc production residues. The selective separation of this element from aqueous solutions using a highly selective process such as SLM can be useful. A SLM process is commonly developed according to a liquid-liquid extraction (LLX) process due to the same mechanism took place in both techniques (Ata 2007). The differences between SLM and LLX systems are as follows: unlike a LLX system, in a SLM process, extraction and stripping processes are carried out in a single stage and a carrier was used within a solid porous membrane is impregnated, as its consumption is less than the amount used in a LLX system. Moreover, easy operation, lower consumption of energy, ease of scaling up, and low investment are the other advantages of SLM systems (Ammari Allahyari et al. 2016; Duan et al. 2017b; Jahanmahin et al. 2016; Swain et al. 2007).

Although there are many investigations on SLM systems, it is still observed a dearth of theoretical information about the importance of SLM in extraction processes (Kaya et al. 2016). In order to know how a SLM process works, theoretical and mathematical modeling based on mass transfer laws governing the SLM systems is applied. A number of studies have been carried out on theoretical modeling of the metal facilitated transport. Most of these models present theoretical values of the diffusion in SLM processes. For instance, mass transfer models of copper(II) in SLM systems using various carriers presented in the literature (Alguacil and Alonso 2005; Alguacil et al. 2001a; Ata 2007; El Aamrani et al. 1999) were used to find transfer parameters. Furthermore, models for the transport of gold species through FSSLM were obtained to find driving forces, rate constants, and diffusional resistances as well as maximum transported metal percentages (Alguacil et al. 2005; Alguacil et al. 2001b; El Aamrani et al. 1998; Sastre et al. 2000). A theoretical model based on Donnan dialysis was used to investigate the diffusion of silver and copper species inside the membrane (Gherrou et al. 2001). Another model developed for the transport of Cr(VI) via FSSLM using Aliquat 336 was applied to determine transport rates and correlated permeability coefficients (Castillo et al. 2002). Furthermore, a kinetic model was developed to evaluate the transport mechanism of cadmium (II) and related diffusional parameters in a

FSSLM system using Cyanex 923 (Alonso et al. 2006). Various models could evaluate kinetic data corresponding to the transport of Cr(VI) in a new developed SLM called Aliquat 336-electric membrane extraction (EME) (Kaya et al. 2016). In a research conducted by Aguilar et al. (2001), the transport of Cd(II) and Pb(II) in a SLM system by the carrier of Kelex 100 was studied, describing the chemical models of the transport with respect to LLX data. The parameters such as the boundary layer thickness and diffusion coefficients were found using these models. Several mathematical models for the facilitated transport of various metals (such as Nd(III), Hg(II), Au(I), Ni(II) etc.) using hollow fiber supported liquid membrane (HFSLM) were also developed in the literature (Alonso et al. 1994; Buachuang et al. 2011; Chaturabul et al. 2015; Danesi 1984; Kumar and Sastre 2000; Prakorn et al. 2006; Prapasawat et al. 2008; Ura et al. 2006; Valenzuela et al. 2002; Wannachod et al. 2014; Yang and Kocherginsky 2007).

In the current study, germanium in the presence of tartaric acid was extracted and transported in LLX and FSSLM processes. In order to know how those occurred, the germanium and tartaric acid complexation should be introduced. There are several studies explained the process of this complexion. According to the literature (Liang et al. 2012; Liu et al. 2010), germanium species in a neutral solution ($GeO_2.H_2O$) can react with tartaric acid and produce $Ge(C_4H_4O_6)_3^{2-}$, meaning that the ratio of tartrate: germanium is equal to 3:1. Since tartaric acid is a weak acid, its hydrolysis descended at very low pHs, resulting in the reduction of the germanium-tartrate formation (Liu et al. 2010). Everest and Harrison (1960) completely investigated the ratio of tartrate to germanium in germanium-tartrate species using adsorption of anionic species on an anion exchanger resin namely Amberlite 400. They reported the formation of 1:1 germanium-tartrate complexes in dilute solutions, converted at pHs< 1.24 to germanium cations and free tartaric acid and decomposed at pHs> 7 due to the reaction of hydroxyl groups with germanium species (Pokrovski and Schott 1998). However, they declared that at a lower concentration of tartaric acid, 2:1 tartrate: germanium species had very similar adsorption results, indicating the formation of 2:1 germanium-tartrate complexes. The formation of the 3:2 tartrate-germanium complex has been predicted at a higher concentration of germanium-tartrate solutions (Everest and Harrison 1960). Vartapetian (1957), Clark and Waddams (1957), Pokrovski and Schott (1998), Pflugmacher and Rohrmann (1957), and Clark (1959) showed that germanium-tartrate species with the ratio of 1:1 were formed at pHs below 6 and decomposed at pHs of 6 to 10; however, they did not present chemical formulas for germanium-tartrate species. Mattock (1954) reported the existence of the 1:1 germanium-tartrate species, and stated this fact that the presence of 2:1

and 1:2 germanium-tartrate could be possible. Sergienko et al. (2010) investigated on the structure of germanium(IV) complexes with tartaric acid prepared in a solution with a pH of 2 and concluded that germanium-tartrate was in the form of $Ge(OH)_2(T)_2^{2-}$. Martsinko et al. (2008) reported the same form of species mentioned in the latter research.

With respect to the aforementioned discussion, probable reactions, which may occur in a solution containing germanium and tartaric acid, are illustrated in Table 1. It is noteworthy that according to various studies (Baes and Mesmer: 1977; Pokrovski et al. 2000), $GeOH_4$ is formed in the neutral medium. In addition, in order to ease and prevent the long writing, T was replaced with $C_4H_4O_6$. As seen in this table, Eqs. (1) and (2) were proposed with respect to the tartaric acid dissociated species, in which the ratio of Ge: tartrate was reported to be 1:1. Furthermore, based on species introduced in the literature (Martsinko et al. 2008; Sergienko et al. 2010), a reaction was proposed as Eq. (3), in which $Ge(OH)_2(T)_2^{2-}{}_{(aq)}$ was formed.

Table 1 The probable reactions between tartrate anions and $GeOH_4$.

Eq.	Reaction	Ge:T ratio	Ge-tartrate reported Ref.
(1)	$Ge(OH)_{4(aq)} + H_3T^-_{(aq)} \Leftrightarrow Ge(OH)_2(HT)^-_{(aq)} + 2H_2O_{(aq)}$	1:1	(Pokrovski and Schott 1998)
(2)	$Ge(OH)_{4(aq)} + H_2T^{2-}{}_{(aq)} \Leftrightarrow Ge(OH)_2(T)^{2-}{}_{(aq)} + 2H_2O_{(aq)}$	1:1	(Pokrovski and Schott 1998)
(3)	$Ge(OH)_{4(aq)} + 2HT^-{}_{(aq)} \Leftrightarrow Ge(OH)_2(T)_2^{2-}{}_{(aq)} + 2H_2O_{(aq)}$	1:2	(Martsinko et al. 2008; Sergienko et al. 2010)

Since the protonated molecules of Alamine 336 (its cationic form) can extract anionic complexes, an acidic solution such as diluted HCl should be used to convert Alamine 336 molecules to their protonated form before experiments. In the reaction written as Eq. (4), Alamine 336 extractant reacts with HCl to produce the protonated species:

$$R_3\,N_{(org)} + HCl_{(aq)} = [R_3\,NH]^+\,[Cl]^-_{(org)} \qquad (4)$$

Knowing the LLX mechanism of the current study using the slope analysis helps choose a proper reaction from Table 1. Eq. (5) shows the probable reaction between the amine extractant and germanium-tartrate species, in which X depicts one of $(T)_2$, (HT), and (T) species shown in Table 1.

$$n[R_3NH^+Cl^-]_{(org)} + Ge(OH)_2X^{n-}{}_{(aq)} \Leftrightarrow [(R_3NH^+)_nGe(OH)_2X^{n-}]_{(org)} + nCl^-{}_{(aq)} \quad (5)$$

Where n shows the number of extractant molecules and the valance of germanium-tartrate anions. As seen in this equation, finding the value of n helps to understand which of the reactions mentioned in Table 1 occurs in the solution. The extraction equilibrium constant (K) of Eq. (5) can be written as Eq. (6)

$$K = \frac{[(R_3NH^+)_nGe(OH)_2X^{n-}]_{(org)}[Cl^-]^n_{(aq)}}{[R_3NH^+Cl^-]^n_{(org)}[Ge(OH)_2X^{n-}]} = \frac{D.[Cl^-]^n_{(aq)}}{[R_3NH^+Cl^-]^n_{(org)}} \quad (6)$$

By taking the log of both sides of Eq. (6) and rearranging, Eq. (7) was obtained:

$$\begin{aligned} &\log(K) = \log(D) + \log[Cl^-]^n_{(aq)} - \log[R_3NH^+Cl^-]^n_{(org)} \Rightarrow \\ &\log(D) = \log K + n\log[R_3NH^+Cl^-]_{(org)} - nLog[Cl^-]_{(aq)} \end{aligned} \quad (7)$$

As seen in Fig. 1, by plotting log(D) as a function of $\log[R_3NH^+Cl^-]_{(org)}$ according to the LLX data obtained in this study, the slope of the line (showing the value of n) was obtained to be 1.8, indicating that 2 moles of extractant have participated in the extraction reaction. Therefore, it can be concluded that one of Eqs. (2) or (3) occurs in the system. This means that only $(T)_2{}^{2-}$ or $(T)^{2-}$ anions exist in the aqueous solution. On the other hand, in the research in which $Ge(OH)_2(T)^{2-}{}_{(aq)}$ was proposed (Pokrovski and Schott 1998), NaOH was added to the germanium-tartrate solution, and the initial pH of the solution was set at 3.49; whereas $Ge(OH)_2(T)_2{}^{2-}{}_{(aq)}$ species reported by Sergienko et al. (2010) was formed in a solution with a pH of 2. Thus, since the condition of the latter research is more similar to that of the current study, it can be concluded that $Ge(OH)_2(T)_2{}^{2-}{}_{(aq)}$ is more probable species formed in the solution. Furthermore, distribution diagrams of tartaric acid show the presence of HT^- at pHs close to 3 (Janjam et al. 2008; Zoecklein et al. 1990). For instance, Fig. 2 illustrates the distribution diagram of tartaric acid constructed by Janjam et al. (2008). As seen in this figure, about 50% of tartaric acid dissociates at the pH range of 2.6-2.7, meaning that there should be 2 moles of HT^- for reacting with $Ge(OH)_4$, resulted in the formation of germanium-tartrate species ($Ge(OH)_2(T)_2{}^{2-}{}_{(aq)}$). Fig. 3 constructed by means of Medusa

153 software confirmed that predominant species (at pHs close to 3) were in the form of
154 $Ge(OH)_2(T)_2^{2-}{}_{(aq)}$. Consequently, the reaction of $Ge(OH)_2(T)_2^{2-}{}_{(aq)}$ with the protonated
155 Alamine 336 in the organic phase can be expressed as Eq. (8):

156 $$2[R_3NH^+Cl^-]_{(org)} + Ge(OH)_2(T)_2^{2-}{}_{(aq)} \Leftrightarrow [(R_3NH^+)_2 Ge(OH)_2(T)_2^{2-}]_{(org)} + 2Cl^-{}_{(aq)} \quad (8)$$

157 In this study, the facilitated transport of germanium using Alamine 336 as a carrier through a
158 FSSLM system was modeled with respect to the flux and the equilibrium equations as well as
159 the Fick's law, solved using the Matlab software. In this regard, in the first step, the extraction
160 equilibrium constant of the extraction reaction based on the LLX data was examined by
161 modeling in Matlab software. The determined constant was used to develop a model for the
162 facilitated transport of germanium species through the FSSLM system. In the facilitated
163 transport model, mass transfer and diffusion coefficients were determined using the coded
164 program. Finally, the performance of the model was evaluated by comparing the calculated
165 and experimental data.

166

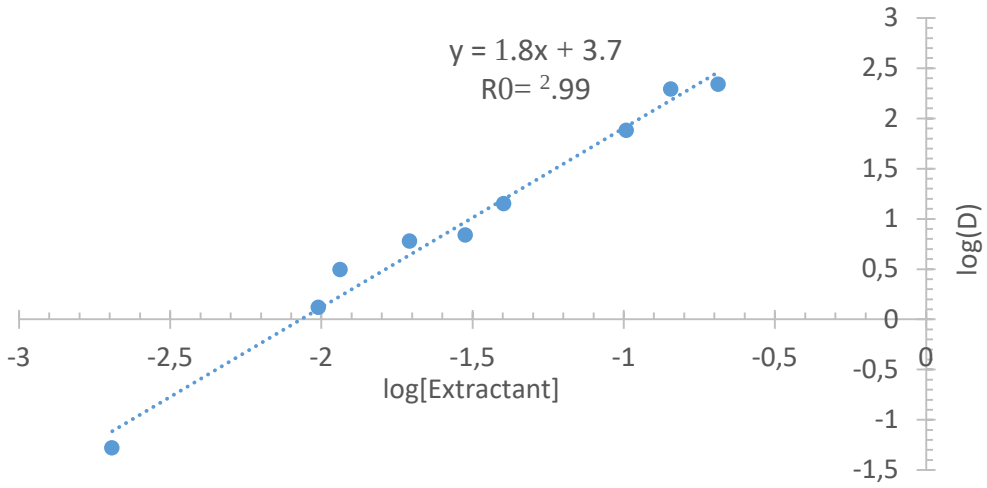

167

168 Fig. 1. Log(D) as a function of $\log[R_3NH^+Cl^-]_{(org)}$ based on Alamine 336 LLX system.

169

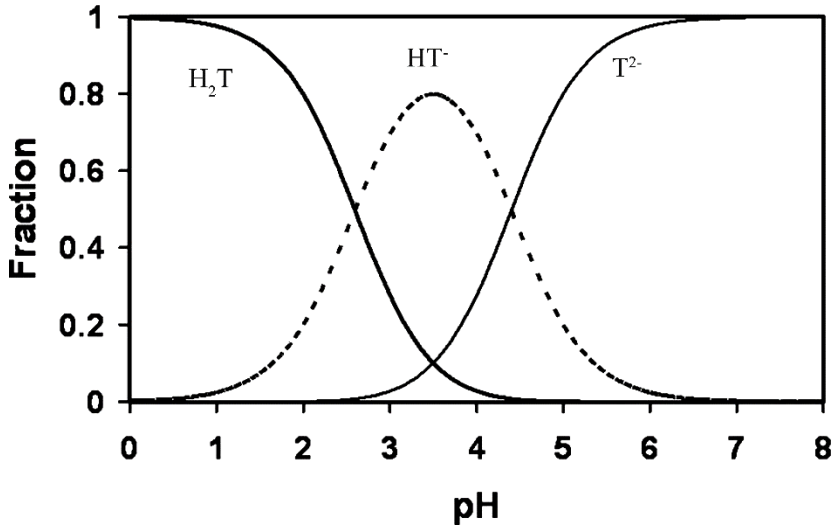

Fig. 2. Distribution diagram of tartaric acid (Janjam et al. 2008).

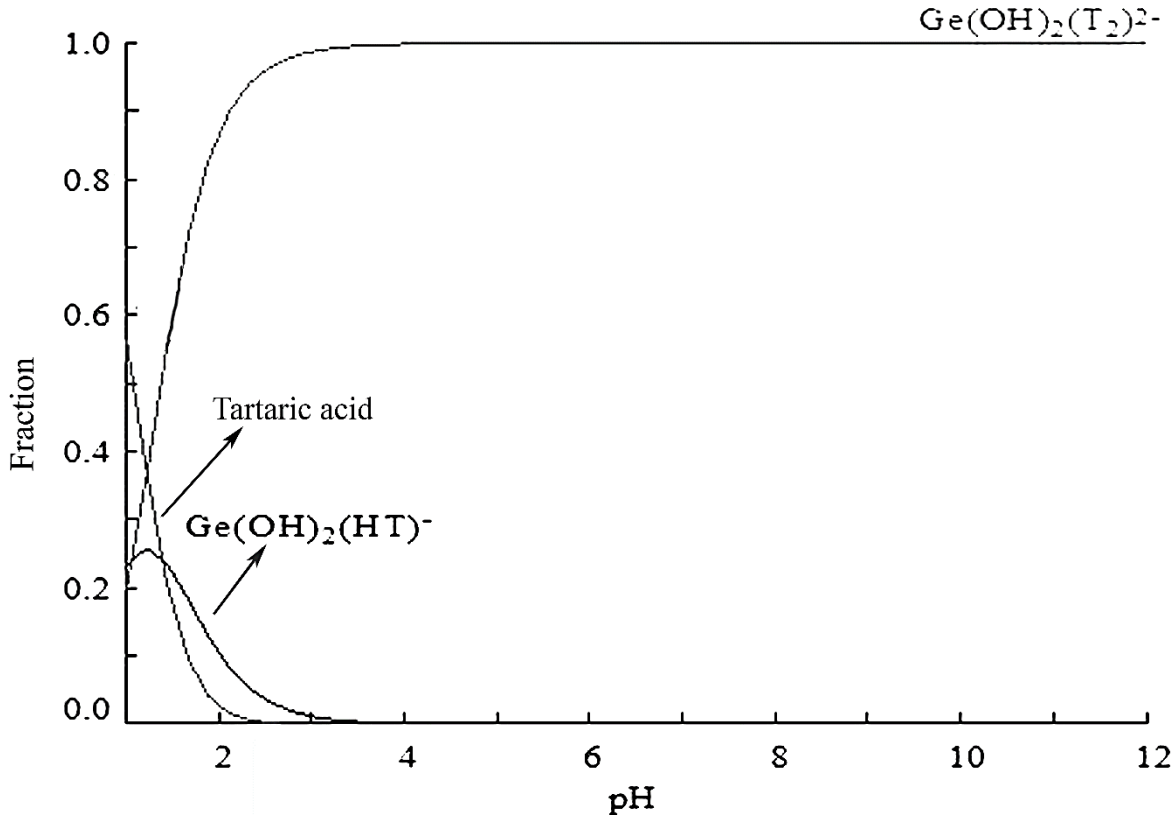

Fig. 3. Speciation diagram of germanium and tartaric acid constructed by Medusa, KTH, Sweden (Ge concentration of 1.378 mmol/Land tartaric acid of 2.760 mmol/L).

Experimental

Materials

Alamine 336 is an anionic exchanger extractant. It is made of tri-octyl/decyl amine, forming organic compounds with anionic aqueous species in an acidic medium. In order to prepare different concentrations of Alamine 336, kerosene from Sigma-Aldrich was used as a diluent. In addition, 10 %v/v of 1-decanol was added as a modifier in the preparation of various concentrations of the extractant. 1-decanol has been suggested as a modifier of organic phases containing various extractants such as Alamine 336 in many studies (Bachmann et al. 2010; Boateng et al. 1989; Fortuny et al. 2014; Marinova et al. 2005). Nakamura and Akiba (1989) declared that the formation of the third phase can be eliminated by adding a long chain alcohol such as 1-decanol to organic extractants. Aqueous solutions containing germanium were prepared by dissolving germanium(IV) oxide with a purity of 99.998 % (Sigma-Aldrich A.C.S. Reagent) in pure distilled water. The other materials used were in AR from Merck, Germany.

Procedures

The first step of modeling in this study was to conduct experiments of the liquid-liquid extraction. The results of these experiments were used to develop a model and find an extraction equilibrium constant. In this regard, a series of experiments was carried out in separatory funnels. In these funnels, equal volumes of organic and aqueous phases (5 mL) were mixed using a mechanical shaker (SBS Instruments SA, Spain) at the room temperature. All the experiments were carried out for 15 min to achieve the equilibrium state. The mentioned phases were separated after each experiment followed by taking an aqueous sample to analyze by an Inductively Coupled Plasma (ICP) apparatus (Agilent 700 Series, US). The concentration of germanium in the organic phase was calculated by mass balancing. The following conditions were obtained according to the optimization experiments found before modeling and used in LLX experiments: the germanium concentration of about 1.378 mmol/L Ge (100 mg/L) in the aqueous phase, the tartaric acid concentration added to the neutral solutions equal to 2.760 mmol/L, 1 M HCl in the strip phases and various Alamine concentrations in the range of 0.1% to 10 %v/v. The initial pH of all aqueous solutions after adding tartaric acid to neutral solutions was between 2.6-2.7. The pH of feed phases descended during the extraction and transport processes. Depending on the Alamine 336 concentration, the equilibrium pH range was observed between 2.1-2.2. In addition, the stripping phase composition was optimized to be 1 mol/L HCl. This concertation was selected as an optimum condition with respect to the experiments conducted at the concentration range of 0.25-2 M. With increasing the HCl concentration up to a certain value, the germanium

transport increases due to the enhancement in the decomplexation of species occurred at the interface of the receiving and membrane phases. On the other hand, at higher concentrations of HCl, the decomposition of transported germanium species are accelerated by reactions in the interfacial levels and takes place promptly. At this condition, the following diffusion of species into the strip phase does not depend on the acid concentration (Duan et al. 2017a).

After conducting the LLX experiments, the flat sheet supported liquid membrane (FSSLM) experiments were performed in a FSSLM apparatus. For each experiment, the membrane of Millipore Durapore poly tetra fluoro ethylene (PTFE) with the diameter of 47 mm, touristy of 1.08, and pore size of 0.45 μm was impregnated in various Almaine 336 concentrations in the range of 0-35 %v/v. The impregnated membrane was rinsed with pure distilled water. The complete description of the FSSLM system used in this research was presented elsewhere (Rathore et al. 2009). This system contained two cells with an operative membrane area of 11 cm^2 (Fig. 4). The feed phase cell with a volume of 220 mL was separated from the strip phase cell with the same volume by a membrane impregnated with Alamine 336 placed in a flanged part. In order to eliminate the influence of residence interfacial films, two impellers in the feed and strip phases were agitated close to the membrane phase at about 1200 rpm. The FSSLM experiments were conducted at the constant values of the parameters reported for LLX experiments.

The kinematic viscosity values of various concentrations of Alamine 336 used in this research were examined by a “Capillary U-Tube Viscometer” by traveling of the carriers via a capillary orifice with the gravity force. The ASTM D445 procedure was used for the mentioned purpose. In order to find dynamic viscosities, kinematic viscosity values multiplied by related densities.

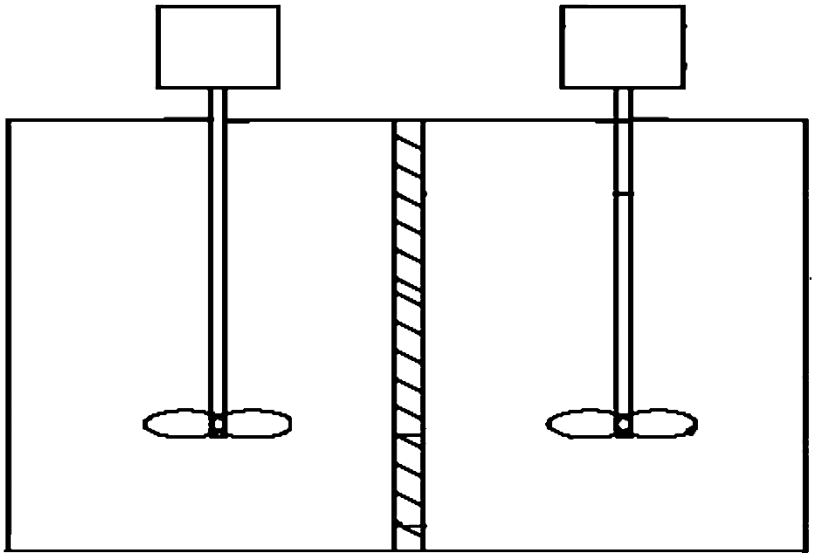

Fig. 4. Schematic illustration of the FSSLM presented in this study (Rathore et al. 2009).

Theory of modeling

Liquid-liquid extraction modeling

In order to develop a LLX mathematical model, the extraction equilibrium reaction equation and the mass balances of species reacted in the liquid-liquid extraction are required. The extraction equilibrium constant can be written as Eq. (9) according to the reaction obtained in Eq. (8):

$$K_{ex} = \frac{[(\mathrm{R_3\ NH^+})_2.\mathrm{Ge(OH)_2(T)_2^{2-}}]_{(\mathrm{org})}.[Cl^-]^2_{(aq)}}{[\mathrm{R_3\ NHCl}]^2_{(org)}.[\mathrm{Ge(OH)_2(T)_2^{2-}}]_{(\mathrm{aq})}} \quad (9)$$

Where org and aq subscripts show the organic and aqueous phases. Eq. (9) forms one of the equations needed to solve the LLX model.

As mentioned, other equations needed to develop a model are mass balances of species shown in Eq. (8). With respect to the organic to aqueous phase ratio (O:A) of 1, the mass balances of germanium and the extractant can be presented as Eqs. (10) and (11), respectively:

$$[\mathrm{Ge}]_{0,\mathrm{i}} = [\mathrm{Ge(OH)_2(T)_2^{2-}}]_{(\mathrm{aq})} + [(\mathrm{R_3\ NH^+})_2.\mathrm{Ge(OH)_2(T)_2^{2-}}]_{(\mathrm{org})} \quad (10)$$

$$[\mathrm{L}]_{\mathrm{total,i}} = 2\times[(\mathrm{R_3\ NH^+})_2.\mathrm{Ge(OH)_2(T)_2^{2-}}]_{(\mathrm{org})} + [\mathrm{R_3\ NHCl}]_{(org)} \quad (11)$$

Where $[Ge]_{0,i}$ and $[L]_{total,i}$ represent the initial concentration of germanium (C_0) and extractant ($L_{total,i}$) in each condition (i). It is noted that (i) refers to various Alamine concentrations (e.g. i=1 denotes 0.1 %v/v Alamine 336). In order to formulize the equations, the concentrations of $[(R_3NH^+)_2.Ge(OH)_2(T)_2^{2-}]_{(org)}$, $[R_3NHCl]_{(org)}$, and $[Ge(OH)_2(T)_2^{2-}]_{(aq)}$ are denoted as *x(1), x(2),* and *x(3),* respectively. These variables are the equilibrium concentrations of species. It is noteworthy that the concentration of chloride ions is equal to two times the concentration of x(1). Therefore, Eqs. (12) to (14) were rewritten using Eqs. (9) to (11) to solve in the mathematical program, respectively:

$$y(1) = K_{ext,j} \times x(2)^2 \times x(3) - 4 \times x(1)^3 \quad (12)$$

$$y(2) = C_{0,i} - x(1) - x(3) \quad (13)$$

$$y(3) = L_{total,i} - x(2) - 2 \times x(1) \quad (14)$$

Where $C_{0,i}$ and $L_{total,\,i}$ denote the initial concentration of germanium and the extractant in each condition (i), respectively. The procedure to find a model for the LLX system was carried out in Matlab R2014b as shown in Fig. 5. As seen in this figure, the liquid-liquid extraction data formed the input data imported to make a data matrix included the number of condition (i), the initial concentrations of Ge and Alamine 336 as well as experimental extraction percentage values. A column was remained blank to save the calculated data in the aforementioned matrix. The percentage of the extraction examined in the model was calculated as Eq. (15):

$$\%E = \frac{C_{Ge,i,org}}{C_{0,i}} \quad (15)$$

Where $C_{Ge,i,org}$ shows the concentration of germanium loaded by the extractant in a specific condition (i). A function responsible for controlling the error between the calculated and experimental data was defined as an Error(x) function calculated as Eq. (16):

$$Error(x) = \sum_{i=1}^{N} (\%E_{cal}(i) - \%E_{i.\exp}(i))^2 \quad (16)$$

Where N is the number of input data. In addition, $\%E_{cal}$ and %Eexp are experimental and calculated extraction percentage values. In order to minimize the objective function of Error(x), *fmincon* Matlab function was used.

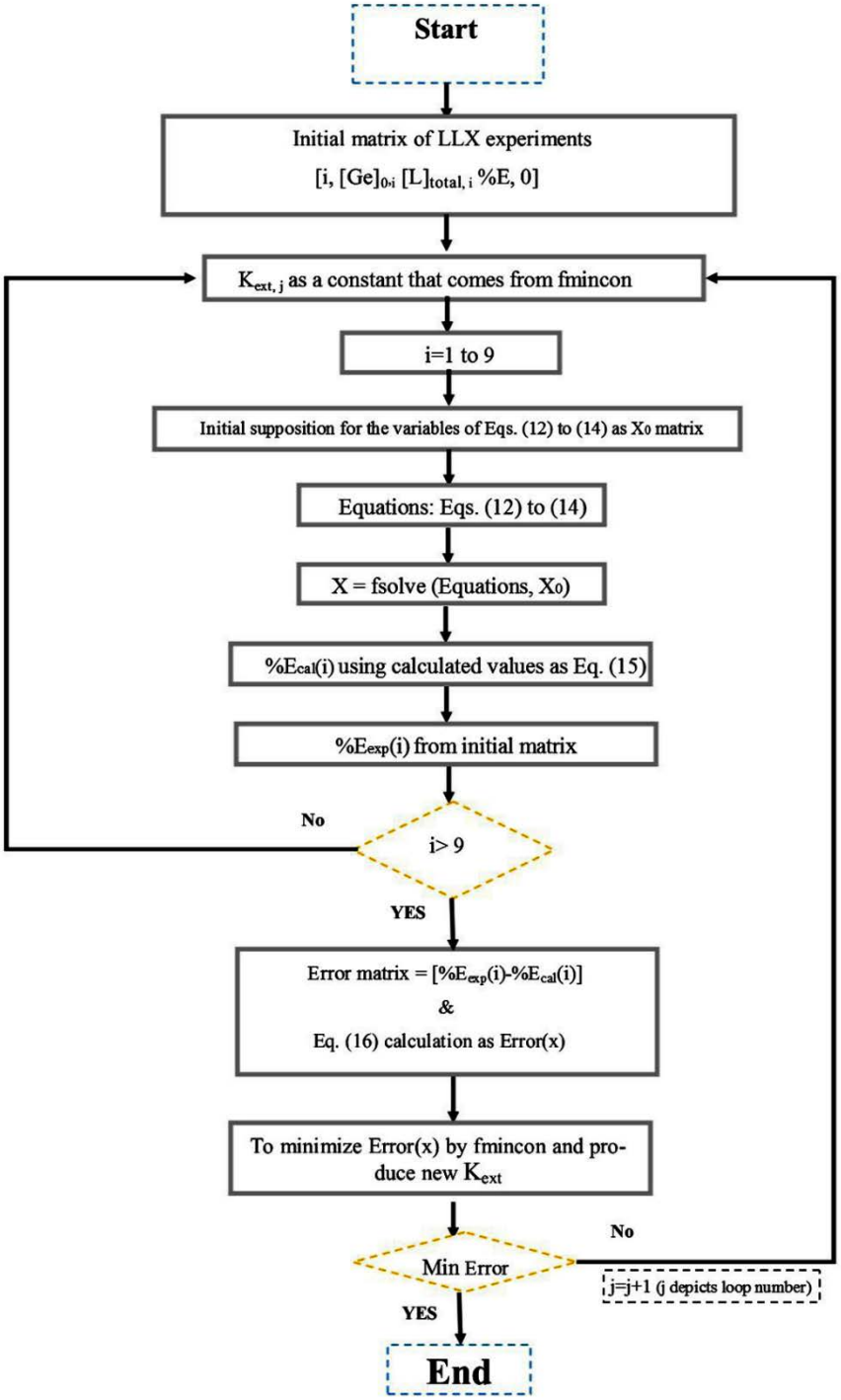

Fig. 5. Schematic diagram of LLX modeling developed by Matlab software.

As shown in Fig. 5, the values of variables in Eqs. (12) to (14) were found in each loop (shown by j) using the *fsolve* Matlab function. According to Eqs. (12) to (14), to solve this system of equations, a value should be dedicated to $K_{ext,j}$. Thus, extraction equilibrium constants were provided by the *fmincon* function in each loop (j). It is noted that modeling was commenced from an initial supposition for the extraction constant called $K_{ext,\ j=0}$. Furthermore, an initial arbitrary supposition for the variables of Eqs. (12) to (14) was required

(as a matrix called X_0). The mentioned loops were continued until the error was minimized. In this condition, the value of K_{ext} was optimized. This optimized value was used in further FSSLM modeling.

SLM modeling

After modeling the liquid-liquid extraction and finding an optimum extraction equilibrium constant, the facilitated transport of germanium through a PTFE membrane impregnated in Alamine 336 was modeled. The overall procedure and functions used in this modeling were similar to modeling developed for the LLX system. The following objects were formed to develop a FSSLM model:

(i) the formation of a matrix with columns containing the condition number (i), the initial concentration of germanium ($[Ge]_{0,\ i}$), the carrier concentrations ($[L]_{total,\ i}$), the number of experimental points in each condition, the number of experimental points (No_{point}) and the viscosity of various carrier concentrations affected the transport.

(ii) the formation of the time matrix with the columns containing the time in which the samples were taken and analyzed for germanium.

(iii) the formation of the concentration matrix including the concentrations of germanium in the feed phase with respect to the experimental points and the time matrix.

It is noteworthy that resistances in the interfacial layers in the feed and strip phases were ignored due to the high-speed agitation of the solution carried out close the membrane phase. According to the literature, the interfacial layer resistances is commonly discounted for rough models (Lantto 2015).

The modeling procedure divided into two series. In the first series, calculations conducted in the inner loop for each condition (i) at different times (t) shown in Fig. 6. (i) is the representative of the Alamine 336 concertation (e.g. i=1 denotes 5 %v/v). The modeling is commenced from an initial arbitrary guess for the mass transfer coefficient and the power of the carrier's viscosity, called $K_{org,0}$ and α_0 (j=0), respectively. In each inner loop, calculations are done for a specific condition (i) at different experimental times (t). It is noteworthy that the calculated germanium concentrations at desired times were saved in a zero matrix shown as $[C(t)]_{Ge,\ f,,\ i}$. After finishing calculations in the inner loop for all the conditions, in the second series of calculations, to determine the error between calculated and experimental values, the error is controlled in the outer loop (countered by j). If the error function is minimized, the calculation will be stopped; otherwise, a new j is dedicated followed by

providing new values for $K_{org,\,j}$ and α_j using fmincon. These series are repeated until the error is minimized. The related equations required for the aforementioned procedure are described as follows:

Modeling was carried out according to the Fick's law of diffusion and flux equations as written in Eqs. (17) and (18), respectively. Since germanium and chloride species were simultaneously transported in an inverse direction, the fluxes and the concentrations of both species should be examined.

$$J_{Ge} = K_{org,j} \times C_{Ge,org,i} \times \mu^{-\alpha} \quad (17)$$

$$J_{Ge} = -\frac{V}{A}\frac{dC_{Ge,f}}{dt} \quad (18)$$

Where J_{Ge} is the flux of species transported across the membrane, K_{org} is an overall mass transfer coefficient related to the diffusion coefficient, μ depicts the viscosity, and α is a constant showing the power of the carrier's viscosity. Furthermore, V is the volume of each reaction cells and A shows an operative area of the membrane. The concentrations of extracted germanium ($C_{Ge,org,i}(t)$) in a specific condition and a certain time was calculated using the concentration of germanium in the feed phase ($C_{Ge,f,i}(t)$) according to an equation obtained from Eq. (9). Thus, $C_{Ge,org,i}(t)$ was found after the resolution of a quadratic equation obtained from Eq. (9) as Eq. (19):

$$C_{Ge,org,i}(t) = ((C_{Cl,f,i}(t)^2 + 4 \times K_{ext} \times L_{total,i} \times C_{Ge,f,i}(t)) - (C_{Cl,f,i}(t)^2 + 4 \times K_{ext} \times L_{total,i} \times C_{Ge,f,i}(t))^2 - (16 \times K_{ext}^2 \times C_{Ge,f,i}(t)^2 \times {L_{total}}^2)^{0.5})/(8 \times K_{ext} \times C_{Ge,f,i}(t)) \quad (19)$$

Where $C_{Cl,f,i}(t)$ is the concentration of chloride anions of the feed phase obtained in each condition and a specific time. The germanium concentration of the feed phase in the time *t* and various experimental conditions (*i)* was obtained using Eq. (18) and rewritten as Eq. (20):

$$C_{Ge,f,i}(t) = C_{Ge,f,i}(t-1) - \frac{A}{V} \times \Delta t \times J_{Ge} \quad (20)$$

Where $C_{Ge,f,i}(t-1)$ is the concentration of germanium in the corresponding time. It is noted that at (t-1)=0, $C_{Ge,f,i}(t-1)$ is equal to the initial concentration of germanium in the feed phase. Moreover, Δt is the range of time in which the calculation is done and in this case is equal to 1 min, meaning that the concentration values are calculated per minute. Furthermore,

350 according to Eq. (8), the transport of chloride from the strip phase to the feed phase is 2 times
351 the germanium transport; thus, the flux of chloride is 2 times the germanium flux.
352 Consequently, the chloride concentration in the feed phase can be obtained using Eq. (21) as
353 follows:

354 $$C_{Cl,f,i}(t) = C_{Cl,f,i}(t-1) + \frac{A}{V} \times \Delta t \times 2J_{Ge} \quad (21)$$

355 In this study, the objective values of $K_{org,j}$ and α_j were searched using *fmincon* function
356 as seen in the flowchart shown in Fig. 6. Similar to LLX modeling, the function responsible
357 for monitoring the error between the calculated and experimental values in each point was a
358 Error(x) introduced in Eq. (16) and rewritten as Eq. (22):

359 $$Error(x) = \sum_{i=1}^{N} (C_{Ge,f,i}(t) - C_{Ge,\exp,i.}(t))^2 \quad (22)$$

360 The modeling process is stopped when the objective error function is in the minimum
361 state.

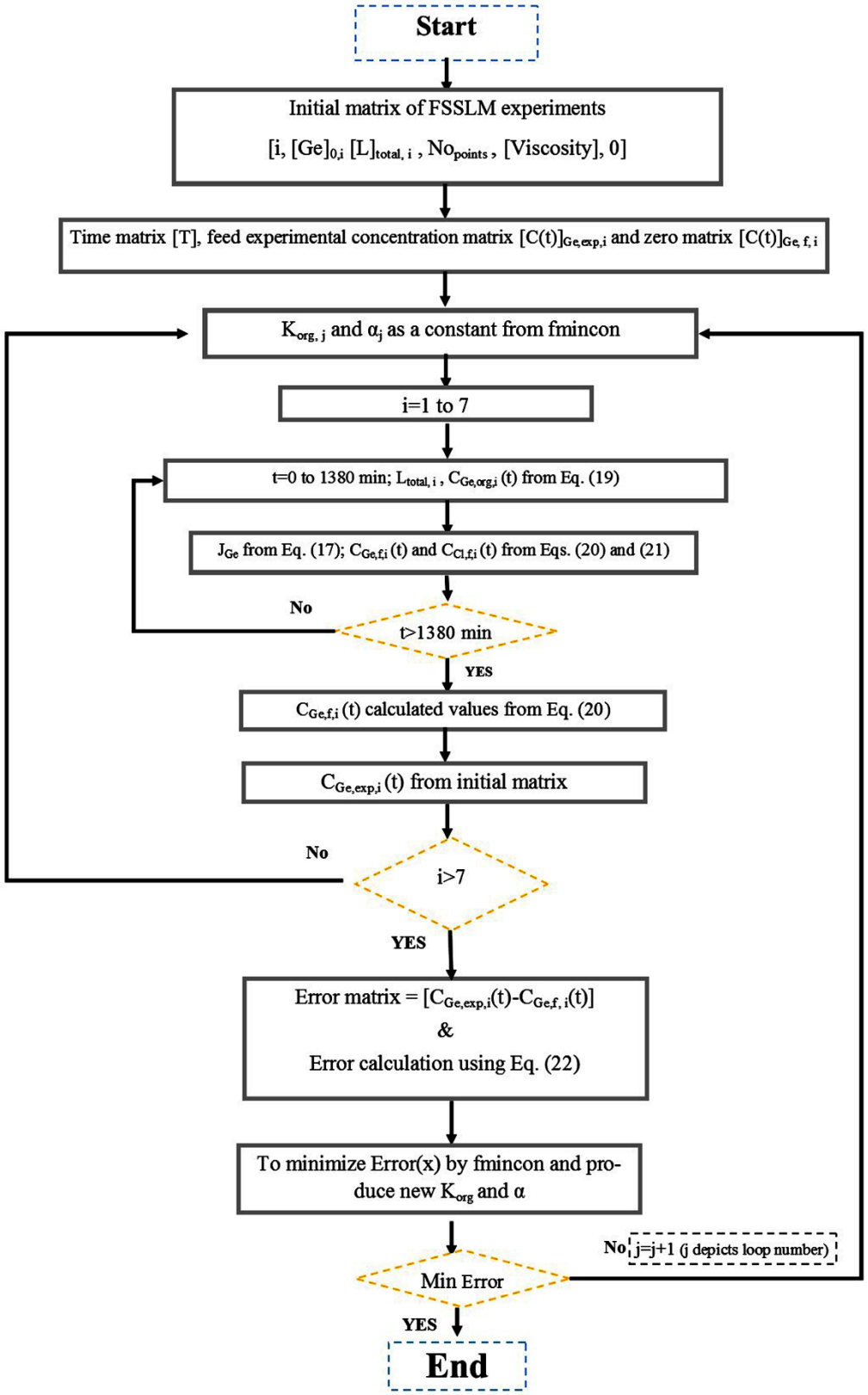

Fig. 6. Schematic diagram of FSSLM modeling developed by Matlab software.

Result and discussion

Liquid-liquid extraction

Mathematical modeling of the LLX system was carried out to find the extraction equilibrium constant that would be used for modeling of the SLM system. Table 2 illustrates the initial conditions of the experiments used for modeling.

Table 2. The initial conditions of the LLX system used for LLX modelling.

Alamine (%v/v)	Alamine (mol/L)	Initial Ge (mmol/L)
10	0.207	1.427
7	0.145	1.427
5	0.103	1.427
2	0.041	1.427
1.5	0.031	1.427
1	0.021	1.427
0.6	0.012	1.427
0.5	0.010	1.427
0.1	0.002	1.427

As shown in Fig. 5, the program was started with the initial matrix of LLX experiments. In order to start the loops, initial conditions required. In this regard, an extraction equilibrium constant was provided by *fmincon* and the matrix of X_0 (included arbitrary values for *x(1), x(2),* and *x(3)*) was defined as a first guess. Eqs. (12) to (14) were solved using *fsolve* for all conditions and new $K_{ext,j}$ was produced in each loop. Finally, *fmincon* found an optimum K_{ext} by which the errors between model and experimental extraction percentages were minimized. According to the result, the optimum value of K_{ext} required for modeling of the FSSLM process was found to be 0.02.

In order to validate the accuracy of the simulated model, the experimental and calculated results (the extraction percentages for each condition i.e. each Alamine 336 concentration) were plotted as Fig. 7. As seen in this figure, the experimental values are perfectly in agreement with the calculated data obtained from the model and the correlation coefficient (i.e. 0.96) confirms this claim. Since there are not any publications in which the equilibrium constant of the germanium extraction by Alamine 336 is calculated, the comparison of the obtained K_{ext} with other values is not possible. Because the PTFE as a

membrane and Alamine 336 as a carrier were used in all experiments, it was anticipated that K_{ext} should be independent of the various experimental parameters such as the extractant concentration etc. A similar claim has been reported in the literature (Kolev et al. 2013).

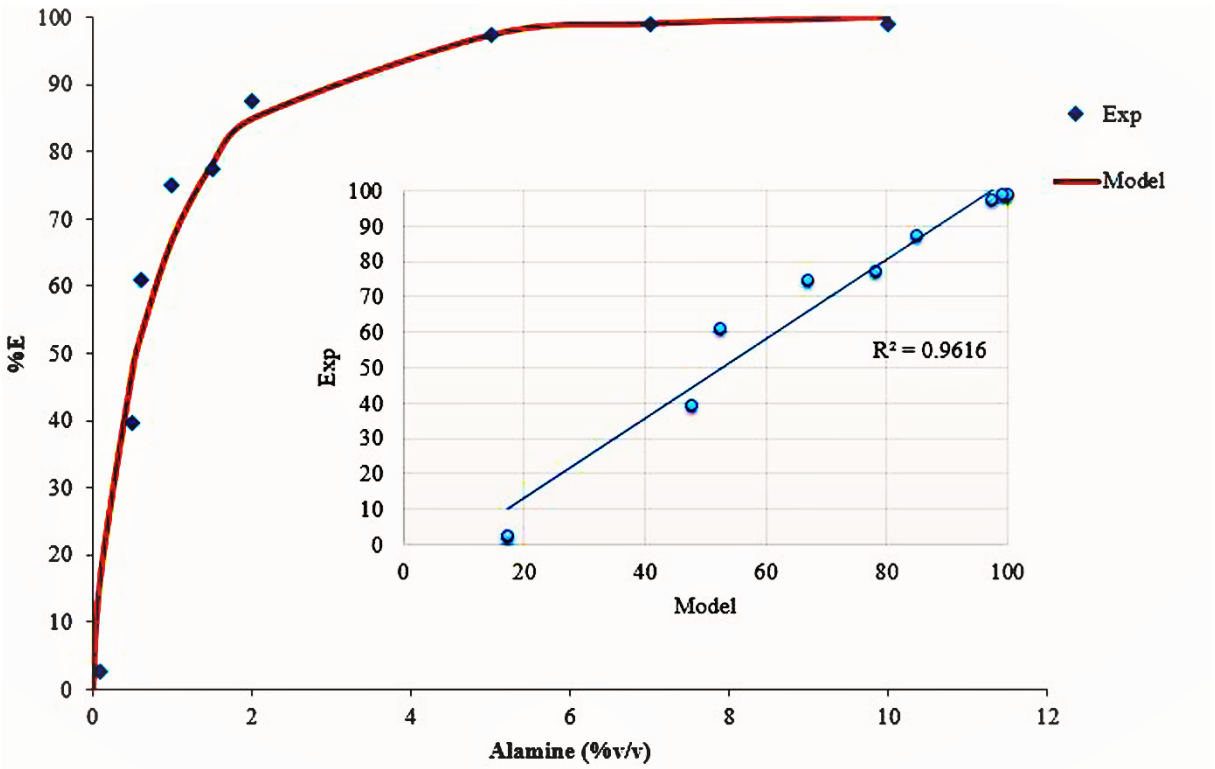

Fig. 7. Comparison of calculated and experimental data of the LLX system in various concentrations of Alamine 336 (%v/v).

Supported liquid membrane

Modeling of the germanium facilitated transport through the liquid membrane containing Alamine 336 was carried out based on the LLX system model and the extraction equilibrium constant found. Table 3 shows the initial conditions used for developing a model for the FSSLM system of this study. The carrier has an essential role in the facilitated transport of species through the membranes (Alguacil et al. 2001a; Ata 2007; Benzal et al. 2004). The aim of this modeling is to find how germanium diffuses through the FSSLM. In this regard, a series of experiments was carried out in various Alamine 336 concentrations in the range of 5-35 (v/v%). In order to monitor the transportation of germanium, the appropriate samples were taken at desired times. The concentration of these samples formed the experimental points, being the base of modeling. Fig. 6 was the road map of mathematical FSSLM modeling performed in Matlab R2014b software. According to this figure, a time loop was considered within the main loop in which the concentration of germanium

corresponding to a specific time in the range of 0-1380 min was calculated. It is noteworthy that only the calculated concentrations corresponding to times in which the samples were taken (experimental points) were stored to compare with experimental concentrations. This comparison was done using the error function as introduced in the theory of modeling section.

Table 3. The initial conditions used for developing a model for the FSSLM of this study.

No. of exp. (i)	Initial Ge (mmol/L)	Alamine (v/v%)	Alamine (mol/L)	Kinematic Vis. (mm^2/s)	Dynamic Vis. (mPa.s)
1	1.249	5	0.103	2.13	1.68
2	1.249	10	0.207	4.84	3.86
3	1.249	15	0.310	8.11	6.50
4	1.249	20	0.414	11.95	9.62
5	1.249	25	0.517	16.37	13.42
6	1.249	30	0.621	21.36	17.52
7	1.249	35	0.724	26.92	22.08

As a result, the overall mass transfer coefficient (K_{org}) and the power of the carrier's viscosity (α) were found to be 5.08×10^{-2} cm/s and 0.66, respectively. The value of 0.66 for the power of the carrier's viscosity (α) is in the agreement with the relationship between diffusion parameters corresponding to high viscose solvents. Hiss and Cussler (1973) implied that the diffusion coefficient in a viscous solvent is proportional to the power of the viscosity, which was reported to be -2/3. This agreement can justify the correctness of the model. According to Eq. (17), since an overall mass transfer coefficient was found by the model, to obtain specific values of mass transfer (called K_m) and the diffusion coefficients (called D_m) corresponding to various carrier concentrations, the values of viscosity, i.e. with the related exponent of -2/3, should be taken into account. Therefore, to find the specific mass transfer coefficients for various concentrations, it must be multiplied by $\mu^{-\alpha}$. Furthermore, the mass transfer coefficient (D_m) was obtained using an equation presented by Prasad and Sirkar (1988) as Eq. (23):

$$K_m = \frac{D_m.\varepsilon}{\delta.\tau} \qquad (23)$$

Where ε, δ, and τ depict porosity, membrane thickness, and tortuosity, respectively. These values were listed in Table 4. The obtained diffusion coefficients (D_m) were compared with the D_m reported in several works in the literature, which investigated the facilitated

transport of various metals and species through a membrane containing Alamine 336. Table 5 illustrates this comparison.

Table 4. The values of viscosity, mass transfer and diffusion coefficients for various concentration of the carrier.

Alamine (%v/v)	μ^{α}	K_m (cm/s)	D_m, (cm^2/s)
5	1.41	3.58×10^{-2}	1.37×10^{-4}
10	2.47	2.05×10^{-2}	7.83×10^{-5}
15	3.50	1.49×10^{-2}	5.53×10^{-5}
20	4.56	1.11×10^{-2}	4.25×10^{-5}
25	5.70	8.92×10^{-3}	3.4×10^{-5}
30	6.81	7.46×10^{-3}	2.84×10^{-5}
35	7.95	6.39×10^{-3}	2.44×10^{-5}

Table 5. The comparison of diffusion coefficients in the literature

Carrier	Solvent	element	Membrane	D_m	ref
Alamine 336 (0.02 M)	Kerosene	Molybdenum(VI)	PTFE	9.61×10^{-6} (cm^2/s) in the aqueous solution	(Marchese et al., 2004)
Alamine 336 (10 %v/v)	TBP	Niobium (V)	Hydrophobic Teflon	9.07×10^{-7} (cm^2/s)	(Campderrós and Marchese, 2001)
Alamine 336 (10 %v/v)	Kerosene	Copper(II) and Cobalt(II)	Microporous Teflon film	2.75×10^{-8} (cm^2/s)	(Marchese et al. 1995)
Alamine 336 (0.18 M)	Kerosene	Molybdenum(VI)	Hollow fiber PTFE contactor	5.08×10^{-6} (cm^2/s)	(Valdés et al. 2009)
Alamine 336 (10 %v/v)	Isopar L Fluid+Pluronic PE 3100	Chromium(VI)	Microporous hollow fiber module	1.38×10^{-3} (cm^2/s)	(Bringas et al. 2006)
Alamine 336 (10 %v/v)	Kerosene+1-Decanol	Germanium(IV)	PTFE	7.83×10^{-5}	This study

As seen in this table, the molybdenum diffusion coefficient in the aqueous phase was found to be 9.61×10^{-6} cm^2/s using the Stoke–Einstein equation by Marchese et al. (2004). The FSSLM system of the mentioned study was contained 0.02 M (≈ 1 %v/v) of Alamine 336 as a carrier in a PTFE membrane with the pore size of 0.45 µm, thickness of 45 µm, and porosity of 0.80. The related mass transfer coefficient was found to be 9.61×10^{-6} cm^2/s. In another FSSLM system developed by Campderrós and Marchese (2001), the facilitated transport of

niobium was studied using Alamine 336 (10 %v/v) diluted in tributyl phosphate (TBP) and a hydrophobic Teflon disc as a membrane with the thickness of 38 μm, pore size of 0.89 μm, and porosity of 0.85. According to this research, the diffusion coefficients in various concentrations of Alamine 336 diluted in TBP was obtained using the Stoke-Einstein equation. The value of diffusion coefficient corresponding to 10 %v/v Alamine 336 was found to be 9.07×10^{-7} cm^2/s. Furthermore, the diffusion coefficient of Co(II), and Cu(II) through a microporous Teflon flat sheet membrane (the thickness of 44 μm, porosity of 87%, and pore size of 1 μm) containing Alamine 336 (10 %v/v) as the mobile carrier was obtained to be 2.75×10^{-8} cm^2/s (Marchese et al. 1995). The mass transport of Mo(VI) has been investigated using a series of resistance models with respect to transport and thermodynamic aspects (Valdés et al. 2009). In the mentioned study, the diffusion coefficient of Mo(VI) across a hollow fiber PTFE contactor with 0.18 M Alamine 336 was found using Stoke-Einstein equation to be 9.31×10^{-8} cm^2/s. The pertraction of Cr(VI) using Alamine 336 and NaOH as the stripping agent across a microporous hollow fiber membrane has been reported by Bringas et al. (2006). According to the result of this study, the organic mass transfer coefficient was found to be 1.5×10^{-3} m/h. Since the diffusion coefficient (D_m) was not calculated in the aforementioned study, this value was calculated to be 1.38×10^{-3} cm^2/s using Eq. (23). This value is higher than that of the other system shown in Table 5. This higher value is due to the greater hollow fiber surface area. According to Table 5, the values of D_m obtained in the current study are higher than those reported in the other studies. In addition, the D_m value of the current study is even comparable with the diffusion coefficient corresponding to the hollow fiber system reported by Valdés et al. (2009). Hence, this result shows the high diffusivity of germanium through the PTFE membrane using Alamine 336.

In order to validate the obtained model, the experimental and calculated values were compared. The experimental data were the extraction percentage of germanium obtained in seven conditions (Alamine 336 concentrations 5, 10, 15, 20, 25, 30, and 35 %v/v). Fig. 8 shows the effect of the carrier concentrations and time on the concentration of germanium in the feed/strip phase for both model (line) and experimental (dash points) data. As seen in these plots, the transport of germanium was carried out through the membrane by prolonging the time until the germanium concentration tended to be zero. Furthermore, Fig. 9 illustrates the plots of the experimental germanium concentrations versus calculated ones. As seen in this figure, the correlation coefficients were found to be 0.99, 0.99, 0.98, 0.97, 1, 1, and 1 for the carrier concentrations of 5, 10, 15, 20, 25, 30, and 35 %v/v, respectively. These values confirm that the modeling concentrations are in good agreement with the experimental data

and show the accuracy of the model. As seen in Fig. 8, the transport rate of germanium in the feed/strip phase increases with increasing the Alamine 336 concentration. According to the extraction model curves, corresponding to the Alamine 336 concentrations of 5, 10, 15, 20, 25, 30, and 35 %v/v, the germanium concentration tended to be zero at the times of 1400, 1100, 1000, 640, 620, 610, and 590 min. These results showed that the transport rate increases at the initial increase of the Almaine 336 concentration and then reaches a steady state. Therefore, at the carrier concentrations above 20 %v/v, there is not a significant change in the transport rate. In the first view, it is assumed that with an enhancement of the Alamine 336 concentration, the transport rate increases. However, this enhancement increases the viscosity resulted in increasing the membrane resistance followed by decreasing the diffusivity of the Ge–amine species through the membrane (see Table 4) (Campderros and Marchese 1994; Marchese et al. 2004). As seen in Table 3, the dynamic viscosity of Alamine 336 increases from 1.68 to 22.08 mPa.s when the Alamine 336 concentration increases from 5 up to 35 %v/v. Since the diffusion coefficient is inversely proportional to the viscosity, this reduction can be justified (Hiss and Cussler 1973). Furthermore, some researchers have attributed this manner to the conductivity of the Alamine 336. At higher concentrations, the conductivity of the carrier reaches a steady state, which affects the transport (Kalachev et al. 1992).

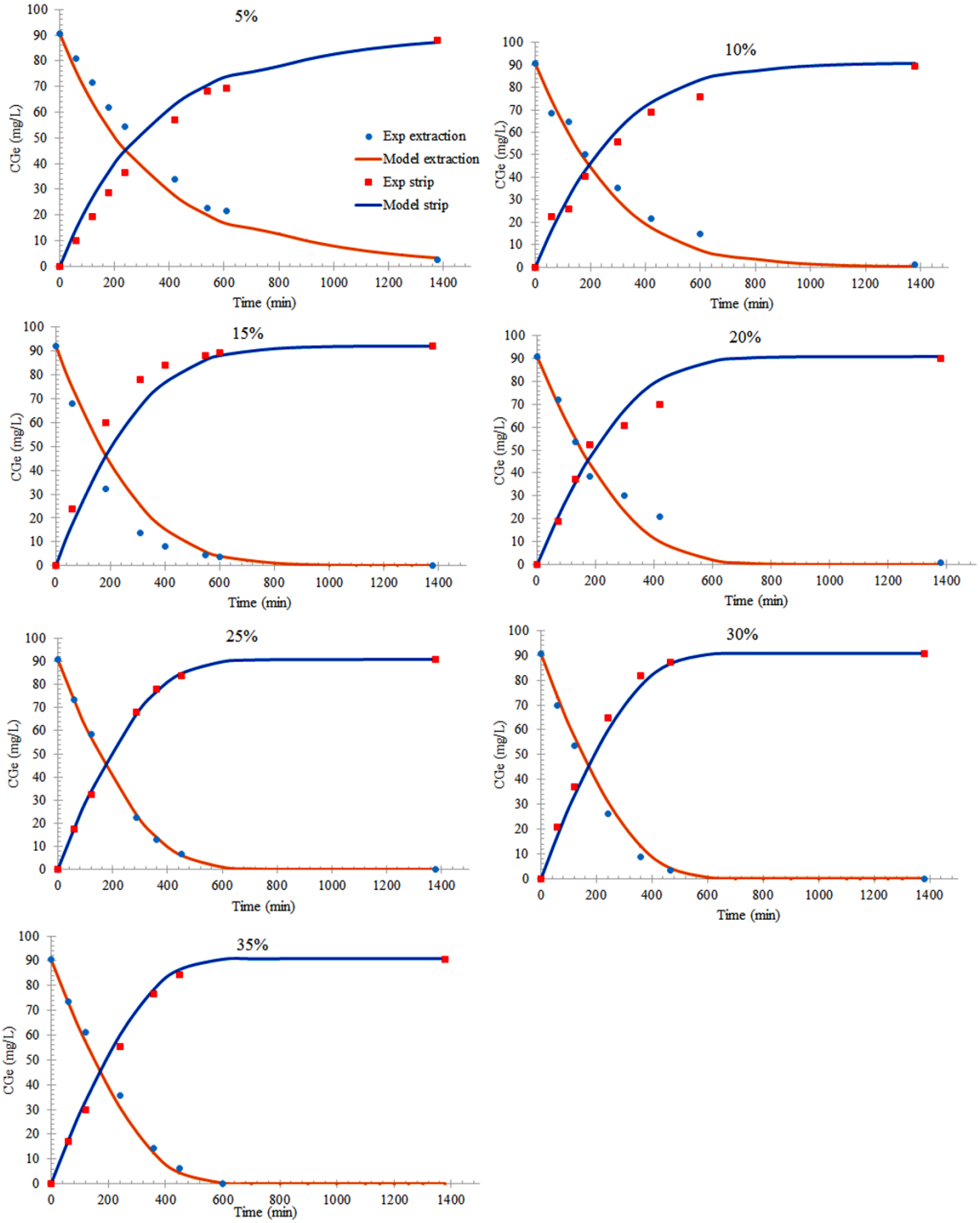

Fig. 8. The effect of the carrier concentrations and time on the concentration of germanium in the feed/strip phase for both model (line) and experiment (dash points) data.

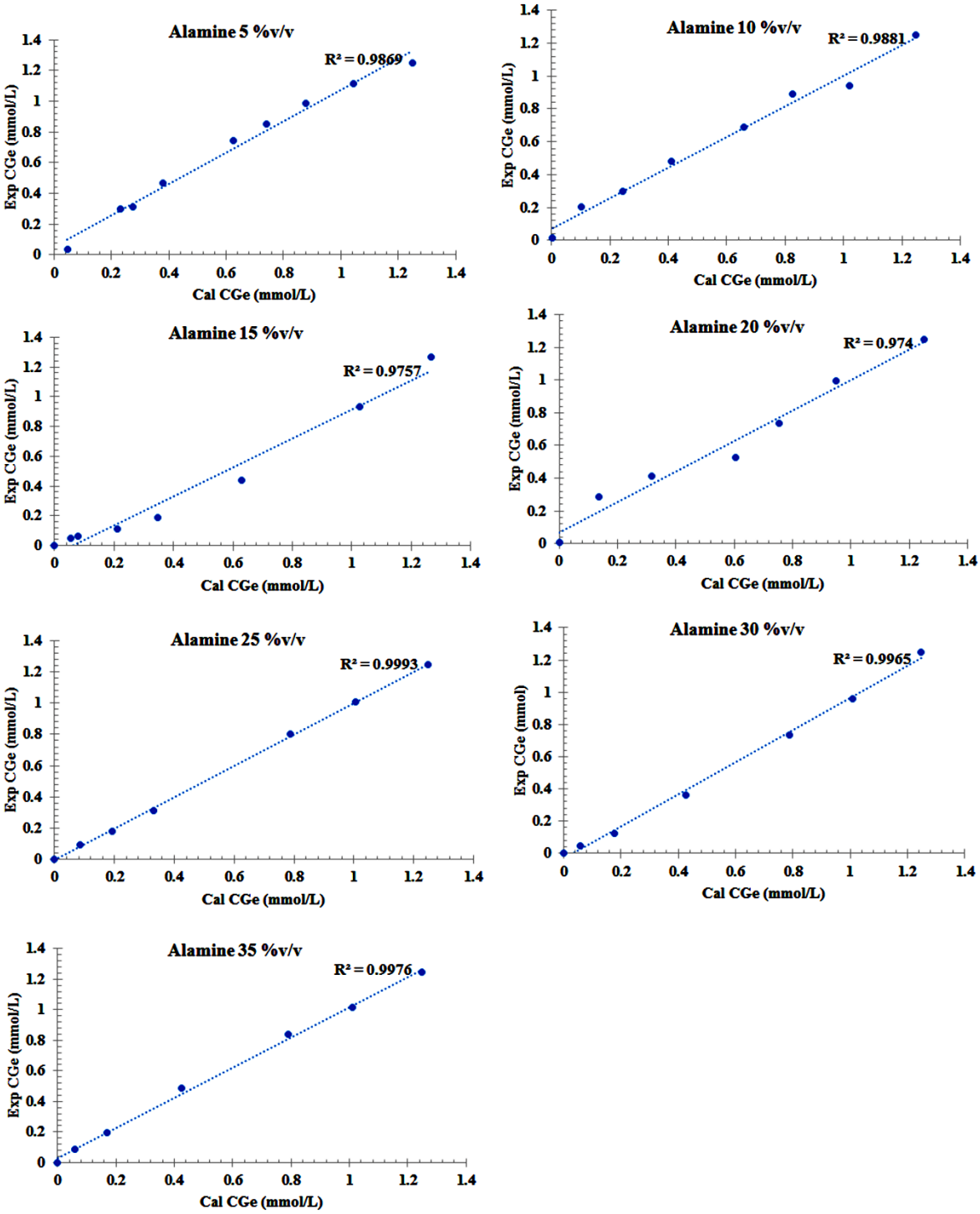

Fig. 9. The experimental germanium concentrations versus calculated ones in various concentrations of Alamine 336.

Conclusions

In this research, a mathematical model was developed based a the LLX model to predict the facilitated transport of germanium from solutions containing tartaric acid through a PTFE membrane containing Alamine 336 as a carrier. The model of the liquid-liquid extraction was developed according to the mass balances and the equilibrium relationship. The LLX model was well fitted to the experimental data. This was resulted in finding the extraction equilibrium constant (K_{ext} = 0.02). This constant was used in further SLM modeling. FSSLM modeling was coded in the mathematical Matlab software with the principle of the flux and the equilibrium equations as well as the Fick's law. As a result, the overall mass transfer coefficient (K_{org}) and the power of the carrier's viscosity (α) were found to be 5.08×10^{-2} cm/s and 0.66, respectively. The obtained value for the power of the viscosity was in agreement with the values reported for viscous solvents in the literature. With respect to the mass transfer and diffusion equations, the specific mass transfer and diffusion coefficients were calculated for different concentrations of the carrier. The obtained diffusion coefficients were compared with the similar values obtained in various systems explained in the literature. Based on this comparison, it can be concluded that the diffusivity of germanium through the PTFE membrane using Alamine 336 is considerable. According to the results, the obtained FSSLM model could be simultaneously fitted to seven sets of the experimental FSSLM data, which were corresponded to Alamine 336 concentrations of 5, 10, 15, 20, 25, 30, and 35 %v/v. The developed models can be useful for further designs and studies on hollow fiber SLM, flat sheet SLM, and LLX systems.

Acknowledgements

This research has been conducted in the laboratory of Department of Chemical Engineering, Universitat Politècnica de Catalunya, Vilanova i la Geltrú Campus, Spain. The authors wish to thank all staffs for their help and suggestions.

References

Aguilar JC, Sánchez-Castellanos M, Rodríguez de San Miguel E, de Gyves J (2001) Cd(II) and Pb(II) extraction and transport modeling in SLM and PIM systems using Kelex 100 as carrier Journal of Membrane Science 190:107-118 doi:http://dx.doi.org/10.1016/S0376-7388(01)00433-1

Alguacil FJ, Alonso M (2005) Description of transport mechanism during the elimination of copper (II) from wastewaters using supported liquid membranes and Acorga M5640 as carrier Environmental science & technology 39:2389-2393

543 Alguacil FJ, Alonso M, Sastre A (2005) Facilitated supported liquid membrane transport of
544 gold (I) and gold (III) using Cyanex® 921 Journal of membrane science 252:237-244
545 Alguacil FJ, Alonso M, Sastre AM (2001a) Modelling of mass transfer in facilitated
546 supported liquid membrane transport of copper(II) using MOC-55 TD in Iberfluid
547 Journal of Membrane Science 184:117-122 doi:http://dx.doi.org/10.1016/S0376-
548 7388(00)00614-1
549 Alguacil FJ, Coedo A, Dorado M, Padilla I (2001b) Phosphine oxide mediate transport:
550 modelling of mass transfer in supported liquid membrane transport of gold (III) using
551 Cyanex 923 Chemical engineering science 56:3115-3122
552 Alonso AI, Urtiaga AM, Irabien A, Ortiz MI (1994) Extraction of Cr (VI) with Aliquat 336 in
553 hollow fiber contactors: mass transfer analysis and modeling Chemical engineering
554 science 49:901-909
555 Alonso M, López-Delgado A, Sastre AM, Alguacil FJ (2006) Kinetic modelling of the
556 facilitated transport of cadmium (II) using Cyanex 923 as ionophore Chemical
557 Engineering Journal 118:213-219 doi:http://dx.doi.org/10.1016/j.cej.2006.02.006
558 Ammari Allahyari S, Minuchehr A, Ahmadi SJ, Charkhi A (2016) Th(IV) transport from
559 nitrate media through hollow fiber renewal liquid membrane Journal of Membrane
560 Science 520:374-384 doi:http://doi.org/10.1016/j.memsci.2016.08.009
561 Ata ON (2007) Mathematical modelling of unsteady-state transport of metal ions through
562 supported liquid membrane Hydrometallurgy 87:148-156
563 Bachmann RT, Wiemken D, Tengkiat AB, Wilichowski M (2010) Feasibility study on the
564 recovery of hexavalent chromium from a simulated electroplating effluent using
565 Alamine 336 and refined palm oil Separation and Purification Technology 75:303-309
566 doi:http://dx.doi.org/10.1016/j.seppur.2010.08.019
567 Baes CF, Mesmer: RS (1977) The Hydrolysis of Cations Berichte der Bunsengesellschaft für
568 physikalische Chemie 81:245-246 doi:10.1002/bbpc.19770810252
569 Benzal G, Kumar A, Delshams A, Sastre AM (2004) Mathematical modelling and simulation
570 of cotransport phenomena through flat sheet-supported liquid membranes
571 Hydrometallurgy 74:117-130 doi:http://dx.doi.org/10.1016/j.hydromet.2004.01.005
572 Bhatluri KK, Manna MS, Ghoshal AK, Saha P (2015) Supported liquid membrane based
573 removal of lead (II) and cadmium (II) from mixed feed: Conversion to solid waste by
574 precipitation Journal of hazardous materials 299:504-512
575 Boateng DAD, Neudorf DA, Saleh VN (1989) Recovery of germanium from aqueous
576 solutions by solvent extraction.
577 Bringas E, San Román MF, Ortiz I (2006) Separation and Recovery of Anionic Pollutants by
578 the Emulsion Pertraction Technology. Remediation of Polluted Groundwaters with
579 Cr(VI) Industrial & Engineering Chemistry Research 45:4295-4303
580 doi:10.1021/ie051418e
581 Buachuang D, Ramakul P, Leepipatpiboon N, Pancharoen U (2011) Mass transfer modeling
582 on the separation of tantalum and niobium from dilute hydrofluoric media through a
583 hollow fiber supported liquid membrane Journal of Alloys and Compounds 509:9549-
584 9557
585 Campderros ME, Marchese J (1994) Membrane transport of cobalt, copper and nickel with
586 trioctyl amine Indian J Chem Technol 1:35-39
587 Campderrós ME, Marchese J (2001) Transport of niobium(V) through a TBP–Alamine 336
588 supported liquid membrane from chloride solutions Hydrometallurgy 61:89-95
589 doi:http://dx.doi.org/10.1016/S0304-386X(01)00165-7
590 Castillo E, Granados M, Cortina JL (2002) Liquid-supported membranes in chromium(VI)
591 optical sensing: transport modelling Analytica Chimica Acta 464:197-208
592 doi:http://dx.doi.org/10.1016/S0003-2670(02)00473-7

Chaturabul S, Srirachat W, Wannachod T, Ramakul P, Pancharoen U, Kheawhom S (2015) Separation of mercury(II) from petroleum produced water via hollow fiber supported liquid membrane and mass transfer modeling Chemical Engineering Journal 265:34-46 doi:http://dx.doi.org/10.1016/j.cej.2014.12.034

Clark ER (1959) Interaction between Organic Hydroxy Acids and Germanic Acid in Aqueous Solution Nature 183:536-537

Clark ER, Waddams JA (1957) Interaction Between Organic Hydroxy Acids and Silicic and Germanic Acids in Aqueous Solutions Nature 180:904-905

Danesi PR (1984) A simplified model for the coupled transport of metal ions through hollow-fiber supported liquid membranes Journal of Membrane Science 20:231-248

Duan H, Wang S, Yang X, Yuan X, Zhang Q, Huang Z, Guo H (2017a) Simultaneous separation of copper from nickel in ammoniacal solutions using supported liquid membrane containing synergistic mixture of M5640 and TRPO Chemical Engineering Research and Design 117:460-471 doi:http://dx.doi.org/10.1016/j.cherd.2016.11.003

Duan H, Yuan X, Zhang Q, Wang Z, Huang Z, Guo H, Yang X (2017b) Separation of Ni2+ from ammonia solution through a supported liquid membrane impregnated with Acorga M5640 Chemical Papers 71:597-606 doi:10.1007/s11696-016-0041-3

El Aamrani F, Kumar A, Beyer L, Cortina J, Sastre A (1998) Uphill permeation model of gold (III) and its separation from base metals using thiourea derivatives as ionophores across a liquid membrane Hydrometallurgy 50:315-330

El Aamrani F, Kumar A, Sastre A (1999) Kinetic modelling of the active transport of copper(II) across liquid membranes using thiourea derivatives immobilized on microporous hydrophobic supports New Journal of Chemistry 23:517-523 doi:10.1039/A901203F

Everest DA, Harrison JC (1960) 747. The chemistry of quadrivalent germanium. Part VIII. Complexes of germanium with tartaric, lactic, and mucic acid Journal of the Chemical Society (Resumed):3752-3758 doi:10.1039/JR9600003752

Fortuny A, Coll MT, Kedari CS, Sastre AM (2014) Effect of phase modifiers on boron removal by solvent extraction using 1,3 diolic compounds Journal of Chemical Technology & Biotechnology 89:858-865 doi:10.1002/jctb.4322

Gherrou A, Kerdjoudj H, Molinari R, Drioli E (2001) Modelization of the transport of silver and copper in acidic thiourea medium through a supported liquid membrane Desalination 139:317-325 doi:http://dx.doi.org/10.1016/S0011-9164(01)00325-3

Hiss TG, Cussler EL (1973) Diffusion in high viscosity liquids AIChE Journal 19:698-703 doi:10.1002/aic.690190404

Hosseini SS, Bringas E, Tan NR, Ortiz I, Ghahramani M, Shahmirzadi MAA (2016) Recent progress in development of high performance polymeric membranes and materials for metal plating wastewater treatment: A review Journal of Water Process Engineering 9:78-110

Jahanmahin O, Montazer Rahmati MM, Mohammadi T, Babaee J, Khosravi A (2016) Cr(VI) ion removal from artificial waste water using supported liquid membrane Chemical Papers 70:913-925 doi:10.1515/chempap-2016-0027

Janjam SVSB, Peddeti S, Roy D, Babu SV (2008) Tartaric Acid as a Complexing Agent for Selective Removal of Tantalum and Copper in CMP Electrochemical and Solid-State Letters 11:H327-H330 doi:10.1149/1.2980345

Kalachev AA, Kardivarenko LM, Platé NA, Bagreev VV (1992) Facilitated diffusion in immobilized liquid membranes: experimental verification of the "jumping" mechanism and percolation threshold in membrane transport Journal of Membrane Science 75:1-5 doi:10.1016/0376-7388(92)80001-Z

642 Kaya A, Alpoguz HK, Yilmaz A (2013) Application of Cr(VI) Transport through the Polymer
643 Inclusion Membrane with a New Synthesized Calix[4]arene Derivative Industrial &
644 Engineering Chemistry Research 52:5428-5436 doi:10.1021/ie303257w
645 Kaya A, Onac C, Alpoguz HK (2016) A novel electro-driven membrane for removal of
646 chromium ions using polymer inclusion membrane under constant D.C. electric
647 current Journal of Hazardous Materials 317:1-7
648 doi:http://dx.doi.org/10.1016/j.jhazmat.2016.05.047
649 Kolev SD, St John AM, Cattrall RW (2013) Mathematical modeling of the extraction of
650 uranium(VI) into a polymer inclusion membrane composed of PVC and di-(2-
651 ethylhexyl) phosphoric acid Journal of Membrane Science 425–426:169-175
652 doi:http://dx.doi.org/10.1016/j.memsci.2012.08.050
653 Kumar A, Sastre A (2000) Hollow fiber supported liquid membrane for the
654 separation/concentration of gold (I) from aqueous cyanide media: modeling and mass
655 transfer evaluation Industrial & engineering chemistry research 39:146-154
656 Lantto J (2015) Analytical model of mass transfer through supported liquid membranes. KTH
657 University
658 Liang J, Fan L, Xu K, Huang Y (2012) Study on Extracting of Germanium with
659 Trioctylamine Energy Procedia 17:1965-1973
660 doi:http://dx.doi.org/10.1016/j.egypro.2012.02.340
661 Liu F, Yang Y, Lu Y, Shang K, Lu W, Zhao X (2010) Extraction of Germanium by the AOT
662 Microemulsion with N235 System Industrial & Engineering Chemistry Research
663 49:10005-10008 doi:10.1021/ie100963t
664 Marchese J, Campderrós M, Acosta A (1995) Transport and separation of cobalt, nickel and
665 copper ions with alamine liquid membranes Journal of Chemical Technology and
666 Biotechnology 64:293-297
667 Marchese J, Valenzuela F, Basualto C, Acosta A (2004) Transport of molybdenum with
668 Alamine 336 using supported liquid membrane Hydrometallurgy 72:309-317
669 Marinova M, Albet J, Molinier J, Kyuchoukov G (2005) Specific influence of the modifier (1-
670 decanol) on the extraction of tartaric acid by different extractants Industrial &
671 engineering chemistry research 44:6534-6538
672 Martsinko EE, Seifullina II, Minacheva LK, Pesaroglo AG, Sergienko VS (2008) Synthesis,
673 properties, and molecular and crystal structure of diantipyrylmethanium Bis(μ-
674 tartrato)dihydroxydigermanate(IV) tetrahydrate (HDAm)2[Ge2(μ-L)2(OH)2] · 4H2O
675 Russian Journal of Inorganic Chemistry 53:1694-1702
676 doi:10.1134/S0036023608110053
677 Mattock G (1954) The complex-forming behaviour of tin, germanium, and titanium with
678 some dibasic carboxylic acids Journal of the Chemical Society (Resumed):989-997
679 doi:10.1039/JR9540000989
680 Mokhtarani B, Khormaei H, Amini MH, Mortaheb HR (2015) Experimental Study on
681 Performance of Modified Hybrid Liquid Membrane Process for Removal of Cadmium
682 from Wastewater Journal of Chemical and Petroleum Engineering 48:109-118
683 Nakamura S, Akiba K (1989) Transport of Europium through Supported Liquid Membrane
684 Containing Dihexyl-N,N-diethylcarbamoylmethylphosphonate Separation Science and
685 Technology 24:1317-1328 doi:10.1080/01496398908050653
686 Peydayesh M, Esfandyari GR, Mohammadi T, Alamdari EK (2013) Pertraction of cadmium
687 and zinc ions using a supported liquid membrane impregnated with different carriers
688 Chemical Papers 67:389-397 doi:10.2478/s11696-013-0310-3
689 Pflugmacher A, Rohrmann I (1957) Über Komplexverbindungen des Germaniums mit
690 organischen Hydroxysäuren Angewandte Chemie 69:778-778
691 doi:10.1002/ange.19570692404

Pokrovski GS, Martin F, Hazemann J-L, Schott J (2000) An X-ray absorption fine structure spectroscopy study of germanium-organic ligand complexes in aqueous solution Chemical Geology 163:151-165 doi:https://doi.org/10.1016/S0009-2541(99)00102-3

Pokrovski GS, Schott J (1998) Experimental study of the complexation of silicon and germanium with aqueous organic species: implications for germanium and silicon transport and Ge/Si ratio in natural waters Geochimica et Cosmochimica Acta 62:3413-3428 doi:http://dx.doi.org/10.1016/S0016-7037(98)00249-X

Prakorn R, Weerawat P, Ura P (2006) Mass transfer modeling of membrane carrier system for extraction of Ce (IV) from sulfate media using hollow fiber supported liquid membrane Korean Journal of Chemical Engineering 23:85-92

Prapasawat T, Ramakul P, Satayaprasert C, Pancharoen U, Lothongkum AW (2008) Separation of As (III) and As (V) by hollow fiber supported liquid membrane based on the mass transfer theory Korean Journal of Chemical Engineering 25:158-163

Prasad R, Sirkar K (1988) Dispersion-free solvent extraction with microporous hollow-fiber modules AIChE journal 34:177-188

Rathore NS, Leopold A, Pabby AK, Fortuny A, Coll MT, Sastre AM (2009) Extraction and permeation studies of Cd(II) in acidic and neutral chloride media using Cyanex 923 on supported liquid membrane Hydrometallurgy 96:81-87 doi:http://dx.doi.org/10.1016/j.hydromet.2008.08.009

Sastre AM, Madi A, Alguacil FJ (2000) Facilitated supported liquid-membrane transport of gold (I) using LIX 79 in cumene Journal of Membrane Science 166:213-219

Sergienko VS, Minacheva LK, Churakov AV (2010) Specific features of the structure of germanium(IV) complexes with polybasic acids Russian Journal of Inorganic Chemistry 55:2001-2030 doi:10.1134/s0036023610130012

Swain B, Jeong J, Lee J-c, Lee G-H (2007) Extraction of Co(II) by supported liquid membrane and solvent extraction using Cyanex 272 as an extractant: A comparison study Journal of Membrane Science 288:139-148 doi:http://dx.doi.org/10.1016/j.memsci.2006.11.012

Ura P, Prakorn R, Weerawat P, Milan H (2006) Feasibility study on the separation of uranium and thorium by a hollow fiber supported liquid membrane and mass transfer modeling JOURNAL OF INDUSTRIAL AND ENGINEERING CHEMISTRY-SEOUL- 12:673

Valdés H, Romero J, Sanchez J, Bocquet S, Rios GM, Valenzuela F (2009) Characterization of chemical kinetics in membrane-based liquid–liquid extraction of molybdenum(VI) from aqueous solutions Chemical Engineering Journal 151:333-341 doi:https://doi.org/10.1016/j.cej.2009.04.012

Valenzuela F, Vega M, Yanez M, Basualto C (2002) Application of a mathematical model for copper permeation from a Chilean mine water through a hollow fiber-type supported liquid membrane Journal of Membrane Science 204:385-400

Vartapetian (1957) Contribution a` l'e´tude des complexes du germanium et de quelques acides a-alcools. Ann Chem 2:917-965

Wang D, Chen Q, Hu J, Fu M, Luo Y (2015) High flux recovery of copper (II) from ammoniacal solution with stable sandwich supported liquid membrane Industrial & Engineering Chemistry Research 54:4823-4831

Wannachod T, Leepipatpiboon N, Pancharoen U, Nootong K (2014) Separation and mass transport of Nd(III) from mixed rare earths via hollow fiber supported liquid membrane: Experiment and modeling Chemical Engineering Journal 248:158-167 doi:http://dx.doi.org/10.1016/j.cej.2014.03.024

Yang Q, Kocherginsky N (2007) Copper removal from ammoniacal wastewater through a hollow fiber supported liquid membrane system: modeling and experimental verification Journal of membrane science 297:121-129

742 Zoecklein BW, Fugelsang KC, Gump BH, Nury FS (1990) Tartaric Acid and Its Salts. In:
743 Zoecklein BW, Fugelsang KC, Gump BH, Nury FS (eds) Production Wine Analysis.
744 Springer US, Boston, MA, pp 289-315. doi:10.1007/978-1-4615-8146-8_13
745
746
747